

## Wave Structure of Liquid Films during the Transition to the Turbulent Flow Mode

A. V. Bobylev<sup>a\*</sup>, S. M. Kharlamov<sup>a</sup>, V. V. Guzanov<sup>a</sup>,  
A. Z. Kvon<sup>a</sup>, and D. M. Markovich<sup>a</sup>

<sup>a</sup> Institute of Thermophysics, Siberian Branch, Russian Academy of Sciences, Novosibirsk, 630090 Russia

\*e-mail: bobylev@itp.nsc.ru

Received February 25, 2019; revised April 25, 2019; accepted April 25, 2019

**Abstract**—The results of an experimental study of the waves on the surface of a vertically falling liquid film in the range of the Reynolds numbers of film flow  $80 < Re < 420$  have been presented. The experiments have been carried out with the use of the field optical diagnostic methods with high spatial and time resolution. Generation of capillary ripples with a small wavelength has been detected at the crests of large three-dimensional waves. It is in these areas of three-dimensional waves where so-called “turbulence spots,” the occurrence of which is associated with a transition to a turbulent flow mode, are observed, as noted in the literature. Long-lived rounded depressions with characteristic transverse dimensions of 1–3 mm, which are formed in the region of the interaction of capillary precursors and then propagate as independent structural elements of the flow, have also been recorded.

**Keywords:** falling liquid film, 3D waves, turbulent flow, laser-induced fluorescence.

**DOI:** 10.1134/S1063785019080078

A smooth transition from the laminar wave mode of flow to the turbulent one occurs in the range of Reynolds numbers  $100 < Re < 400$  [1] according to modern concepts for vertically falling liquid films. Here,  $Re = q/\nu$ ,  $q$  is the specific volume flow rate and  $\nu$  is the kinematic viscosity. The modes that correspond to the  $Re$  range from 50 to 1000 are, as a rule, implemented in industrial plants where the film flow occurs [2]. Thus, the features of the flow modes that are transitional to turbulence should have a significant impact on the efficiency of the operation of equipment. At the same time, the wave characteristics of liquid films at transitional modes have not been studied in sufficient detail due to technical limitations of measurement methods and complex three-dimensional (3D) wave structure of the flow. The use of field measurement methods provides great opportunities for the study of three-dimensional wave modes of the film flow and, accordingly, allows the refinement of the existing classification of the flow modes depending on the Reynolds number and geometric parameters of the problem. Currently, the two-dimensional (2D) flow modes in various geometry, including vertically falling film, have been described in detail using the widely used shadow visualization method along with local measurement methods [1]. The scenarios of

transition from 2D- to 3D-wave modes of film flow were studied for the cases of inclined and vertical plates using the field method of the fluorescent visualization and its modification—the method of laser-induced fluorescence (LIF) [3, 4]. Detailed information on various structural elements of wave fields was obtained and classification of 3D wave flow modes for Reynolds numbers  $Re < 100$  has been performed in a number of works [5–7] using the field measurement methods. However, very few experimental works in which the wave structure of the film in the transition to the turbulent flow mode is investigated by the field methods can be found in the literature. One such publication is [5], in which flow modes on a vertically falling liquid film at  $27 < Re < 200$  were investigated. The flare spots were found on the crests of large 3D waves at  $Re > 70$  by the method of fluorescent visualization in [5]. The authors explained this phenomenon as being due to the existence of “turbulence spots” in these areas, where the film surface has large inclination angles with respect to the channel wall due to its turbulization, which leads to flares in the measuring system used by the authors. The frequency of the flare spots, their number and size increase with the increasing of the Reynolds number. The authors of [5] used an arrangement of the optical system in which the

excitation and recording of the fluorescence are implemented from the side of the transparent wall, on the opposite side of which the film flows. The flare in this arrangement is due to the focusing of the reflected light under the wave surface of the film or occurs in those areas where the slope of the free surface of the film approaches the angle of the total internal reflection or exceeds it. The wave structure of these spots remains unexplored due to the limitations of the fluorescent visualization method at this arrangement, and flare areas are considered to be the regions of turbulent flow, with the appearance and further growth of which the transition to the turbulent film flow begins [5, 8]. In this regard, a natural question arises about the study of the wave structure of “turbulence spots.” The objective of this work is an experimental study of the wave surface of the film at the transitional flow modes in which there are “turbulence spots.”

The experiments were performed on a transparent vertical plate  $45 \times 140$  cm in size (a detailed description of the installation can be found in [7]) and on the outer surface of the vertical cylinder with a diameter of 60 mm and a height of 150 cm. The film flow modes with a natural wave evolution on water and on 25% water–glycerin solution (WGS) with density  $\rho = 1.06 \text{ g/cm}^3$  and  $\nu = 1.7 \times 10^{-2} \text{ cm}^2/\text{s}$  in the range of the Reynolds numbers  $80 < \text{Re} < 420$  were studied. We used high-speed field methods LIF and shadow visualization were used in [7]. They were used to obtain the general flow patterns along the entire length of the operational area (shadow method) and local distributions of the film thickness in the areas ranging in size from  $4 \times 13$  to  $15 \times 15$  cm with a resolution of 0.13 mm per pixel at the distances from the slit film-former up to 1.4 m (by the LIF method). The flow was captured by a high-speed camera with a frequency of 1 kHz, exposure time of 1 ms, and shooting time of 2 s in all cases, which made it possible to observe the dynamics of the features of the wave evolution of the studied modes. The LIF method was used, and Rhodamine 6G was dissolved in the operational liquid in quantities of 20–30 mg/L, the fluorescence of which was excited by a continuous green laser. The illumination and recording were carried out from the side of the free surface of the film in contrast to [5], which made it possible to get rid of a number of factors leading to the flare of the obtained images. The cases of total internal reflection of light inside the liquid film do not occur when the layout of the measuring system proposed by us is used and focusing under the wave surface of the film occur at distances that are seven to eight times greater than in [5], which allows resolving the small scale structure arising on the crests of large waves without significant distortions.

The comparison of the wave patterns for the cases plate and cylinder showed that the type of the working area does not affect the wave structure of the flow.

Minor differences in the wave flow modes for the cases of water and WGS are mainly expressed in the fact that the same modes are realized at higher values of the Reynolds number for WGS ( $\Delta \text{Re} \approx 20$ ).

The appearance of new structural elements of the wave pattern in comparison with those described in [7] becomes noticeable at  $\text{Re} \approx 150$ . Although the main element of the wave structure is still the 3D waves chaotically interacting between themselves when the Reynolds number increases, the appearance of these waves itself begins to change at  $150 < \text{Re} < 220$ . While all crests of the 3D waves remain smooth at lower Re (Fig. 1a), an increase in Re leads to the appearance of 3D waves the main crest of which is covered with capillary ripples (Fig. 1b). The capillary ripples on the surface of 3D waves occur, as a rule, due to their interaction with small disturbances on the residual layer. After having been occurred, such ripples, having a regular striped or cellular structure with a wavelength of 1–2 mm, quickly capture most of the wave surface and move to its back slope, fading at the same time. The ripple has a lifetime of a few hundredths of a second. The wave crest becomes smooth after its decay. The maximum amplitude of the capillary ripple is recorded at the level of 0.25 mm for a characteristic value of the film thickness in the wave crest of 0.9–1.1 mm at the region of  $\text{Re} \sim 200$ . The capillary structures at the crests of the 3D waves begin to lose the regularity at a further increase in the Reynolds number (Fig. 1c). Their maximum amplitude is reduced to 0.1 mm. Waves that interact with disturbances on the residual layer or with each other occur so often that capillary ripples from the previous disturbance that have time to fade. As a result, the surface of such waves is covered with chaotic ripples and takes the form of the areas occupied by the turbulent motion of the liquid. These areas do not distinguished by spectral processing against the background of the capillary precursors, capturing large areas of the smooth film surface between large waves: they make a small contribution to the same spectral region as the waves of the capillary precursor.

Once the  $\text{Re} > 400$  modes are reached, the surface of the vast majority of 3D waves is covered with chaotic capillary ripples, which can be considered a sign of transition to a hydrodynamic turbulence.

The formation of a system of depressions of round shape—“craters” with transverse dimensions of 1–3 mm (Fig. 2) arising in the regions of the interaction of the capillary precursor of the neighboring 3D waves—is also an interesting feature in the studied range of Re. After being formed, such structures move along the residual layer as independent elements and disappear in the process of the interaction when encountering a 3D wave. The characteristic lifetime of the “craters” is 0.1 s. The film thickness in their center is 0.2–0.3 mm less than in the surrounding liquid according to the LIF measurements.

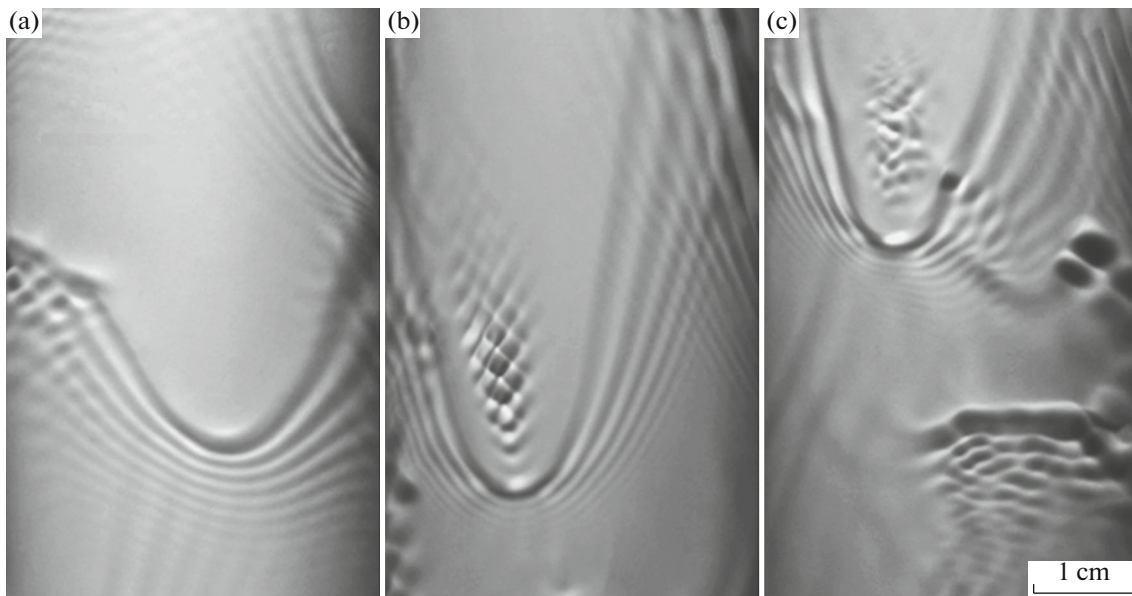


**Fig. 1.** Shadow images of three-dimensional waves in the region of the steady-state flow at a distance of 80 cm from the distributor, WGS. (a) 3D wave with a smooth crest at  $Re = 80$ , (b) cellular structure on the surface of a 3D wave at  $Re = 190$ , and (c) blurring of the cellular structure at  $Re = 220$ .

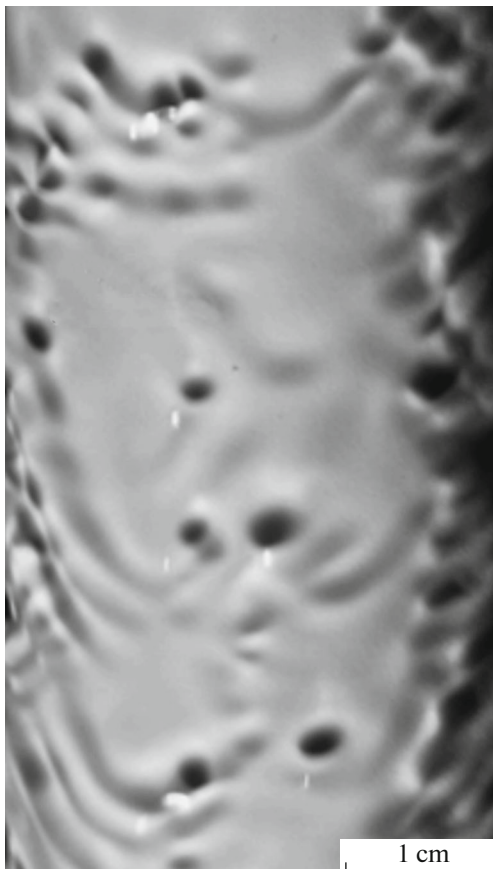


**Fig. 2.** The system of deep depressions on the surface of the film, resulting from the interaction of the capillary precursors of 3D waves, WGS,  $Re = 220$ .

Thus, the analysis of experimental data shows that the transition to the usual hydrodynamic turbulence can begin with the generation of high-frequency capillary ripples on the surface of individual 3D waves at the film liquid flow. As for another type of small-scale structures—“craters” with a reduced thickness of the residual layer—their influence on the wave processes is not obvious. On the one hand, they are an additional source of disturbances leading to the appearance of capillary ripples on large waves. On the other hand, although their number increases with the Reynolds number, it remains rather small compared to other sources of disturbances in the studied range. Perhaps their role will manifest itself with a further increase in the Reynolds number.

#### FUNDING

The work was carried out within the framework of a state order to the Institute of Thermophysics, Siberian Branch, Russian Academy of Sciences, and with the financial support of the Russian Foundation for Basic Research, project no. 18-01-00682.

#### CONFLICT OF INTEREST

The authors declare that they have no conflict of interest.

#### REFERENCES

1. S. V. Alekseenko, V. E. Nakoryakov, and B. G. Pokusaev, *Wave Flow of Liquid Films* (Nauka, Novosibirsk, 1992) [in Russian].

2. S. Mukhopadhyay, M. Chhay, and C. Ruyer-Quil, in *Proceedings of the 23eme Congres Francais de Mecanique, Lille, France, 2017*.
3. J. Liu, J. B. Schneider, and J. P. Gollub, *Phys. Fluids* **7**, 55 (1995).
4. S. M. Kharlamov, V. V. Guzanov, A. V. Bobylev, S. V. Alekseenko, and D. M. Markovich, *Phys. Fluids* **27**, 114106 (2015).
5. P. Adomeit and U. Renz, *Int. J. Multiphase Flow* **26**, 1183 (2000).
6. C. D. Park and T. Nosoko, *AIChE J.* **49**, 2715 (2003).
7. V. V. Guzanov, A. V. Bobylev, O. M. Hienz, S. M. Kharlamov, A. Z. Kvon, and D. M. Markovich, *Int. J. Multiphase Flow* **99**, 474 (2018).
8. E. A. Demekhin, E. N. Kalaidin, S. Kalliadasis, and S. Y. Vlaskin, *Phys. Fluids* **19**, 114103 (2007).

*Translated by N. Petrov*